# A Normalized Metric for Effective Atomic Number Estimation in Dual-Energy X-Ray Imaging

**Author:** Grégory Jean

**Keywords:** DECT, Z-Image, Dual-Energy X-Ray, Material Discrimination

**Abstract:**
Dual-energy X-ray imaging generates Z-images to classify materials and estimates the effective atomic number ($Z_{eff}$) to identify specific organic substances such as explosives or narcotics. Conventional methods relying on the attenuation ratio $R = \frac{\mu_1}{\mu_2}$ exhibit limited sensitivity for distinguishing materials with close $Z_{eff}$ values, such as TNT and water. This study introduces a normalized metric $M=\frac{\mu_1-\mu_2}{\mu_1+\mu_2}$, transposed from the Michelson contrast index used in satellite remote sensing, and evaluates its performance through analytical simulation on 15 organic materials (Z_eff ranging from 5.4 to 8). Simulated spectra centered at 60keV and 120keV with $10^4$ events per spectrum are based on Jia Hao et al. (2013). Results show a relative error of ±3.51 % for M compared to ±4.56 % for R, a 23 % reduction in estimation error, demonstrating M's enhanced sensitivity to $Z_{eff}$ variations in the organic domain. Error propagation analysis confirms that $\Delta M < \Delta R$ for $R \in [0.7, 0.9]$. These findings illustrate that elementary transformations of existing dual-energy measurements remain underexplored, and that meaningful gains in material discrimination are accessible without modifying acquisition hardware or resorting to iterative reconstruction methods.

## Introduction

Dual-energy X-ray imaging leverages energy-dependent attenuation properties to estimate the effective atomic number ($Z_{eff}$) of materials, enabling their differentiation in fields such as medical imaging and security screening. By acquiring attenuation data at two distinct energy levels (typically low $E_1$ and high $E_2$), this technique exploits the predominance of the photoelectric effect ($\propto Z^3/E^3$) and Compton scattering (Klein-Nishina formula) to distinguish materials based on $Z_{eff}$ and density.

The state-of-the-art builds on foundational work by Alvarez and Macovski (1976), who modeled attenuation as a linear combination of photoelectric and Compton contributions:

$$\mu(E) = a_1 \cdot f_{pe}(E) + a_2 \cdot f_c(E)$$

In practice, the attenuation ratio $R = \frac{\mu_1}{\mu_2}$ (where $\mu_1 = \mu(E_1)$ and $\mu_2 = \mu(E_2)$) is widely employed in security systems (Yalçın, 2022) to minimize dependencies on material density ($\rho$) and thickness ($l$). Alternative approaches, differential attenuation, material basis decomposition, iterative reconstruction, exist and have been extensively developed over the past two decades. Yet despite this breadth of algorithmic effort, a simpler question has received comparatively little attention: are there elementary transformations of the two measured attenuation values that outperform R without requiring any additional acquisition or computation?

This question is the starting point of the present note. Algorithmic development in dual-energy CT has been dominated by reconstruction-side complexity, iterative solvers, regularisation schemes, neural network architectures, while the measurement-side representation of the two channels has remained largely unchanged since the introduction of R. The present work

examines whether a simple normalisation, absent from the dual-energy X-ray literature, can improve $Z_{eff}$ discrimination in the organic domain at no additional cost.

The metric under consideration, $M=\frac{\mu_1-\mu_2}{\mu_1+\mu_2}$, is transposed from the Michelson contrast index used in satellite remote sensing to reduce measurement noise. Although undocumented in the context of dual-energy X-ray imaging, its formulation, normalising the attenuation difference by the sum rather than by a single channel, is grounded in established contrast normalisation principles and warrants evaluation for CT applications. The relationship $M = \frac{1-R}{1+R}$ shows that M is a direct transform of R, preserving all physical information while modifying the sensitivity profile across the $Z_{eff}$ range.

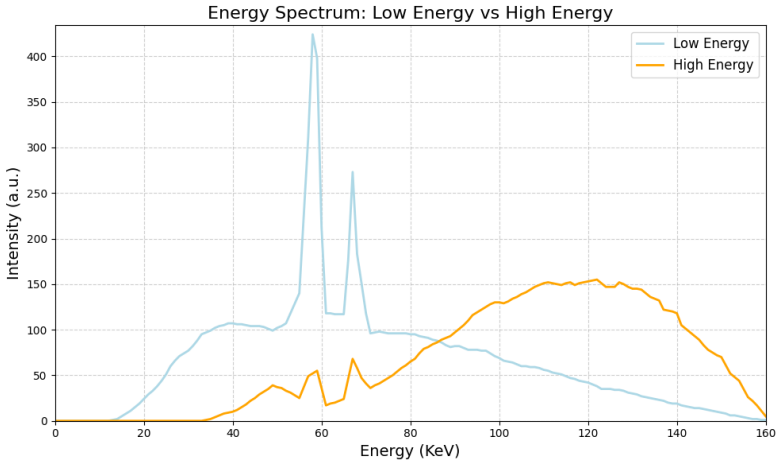


*Figure 1: Energy distribution of the two spectra used for calculations, centered at 60keV and 120keV, adapted from Jia Hao et al. (2013).*

## Hypotheses and Methodology

We hypothesize that $M=\frac{\mu_1-\mu_2}{\mu_1+\mu_2}$ outperforms $R=\frac{\mu_1}{\mu_2}$ in estimating $Z_{eff}$ for organic materials due to its normalization. The formulation of M resembles the Michelson contrast index: $\frac{I_{max}-I_{min}}{I_{max}+I_{min}}$, suggesting a heuristic approach to optimize material separation. Literature typically employs three expressions to estimate $Z_{eff}$:

1/ Attenuation ratio: $R=\frac{\mu_1}{\mu_2}$, where $Z_{eff} = f(R)$ via calibration curves (Yalçın, 2022).

2/ Differential attenuation: $\Delta\mu=\mu_1-\mu_2$, often normalized as $Z_{eff}=f(\frac{\mu_1-\mu_2}{\mu_1})$.

3/ Basis decomposition: $\mu(E)=\rho_1\cdot\mu_{base1}(E) + \rho_2\cdot\mu_{base2}(E)$ for two materials.

Recent studies introduce compensatory coefficients derived from additional variables to correct scanner-specific effects. Our metric, $M=\frac{\mu_1-\mu_2}{\mu_1+\mu_2}$, aligns with differential methods but features a symmetric denominator.

Performance comparison utilizes spectra from Jia Hao et al. (2013), Figure 1, centered at 60keV and 120keV. An analytical model, based on NIST data extrapolation, calculates probable photon attenuation, uniformly distributed across the spectra, assuming 50% Compton scattering contribution. Interactions with 15 organic materials ($Z_{eff}$ 5.4–8, Table 1) are computed for a

constant 2 cm thickness. Performance is assessed by the relative precision of $Z_{eff}$ prediction against a linear extrapolation derived from 15 data points (Figure 2).

| N° | Material | Chemical Formula | Zeff | R | D |
|---|---|---|---|---|---|
| 1 | Petrol | C8H18 | 5,39 | 0,8691 | -0,0700 |
| 2 | ABS | C15H17N | 5,76 | 0,8633 | -0,0734 |
| 3 | Oil | C18H34O2 | 5,83 | 0,8576 | -0,0767 |
| 4 | Canabis | C21H30O3 | 6,02 | 0,8515 | -0,0802 |
| 5 | Alcohol | C2H5OH | 6,35 | 0,8402 | -0,0868 |
| 6 | Cocaine | C17H21NO5 | 6,41 | 0,8420 | -0,0858 |
| 7 | Coffe | C8H10N4O2 | 6,51 | 0,8299 | -0,0930 |
| 8 | PET | C10H8O4 | 6,64 | 0,8370 | -0,0887 |
| 9 | Cotton | C6H10O5 | 6,89 | 0,8168 | -0,1009 |
| 10 | Sugar | C12H22O11 | 6,92 | 0,8220 | -0,0977 |
| 11 | Honey | C6H12O6 | 6,95 | 0,8269 | -0,0947 |
| 12 | TNT | C7H606N3 | 7,04 | 0,8259 | -0,0953 |
| 13 | Muscle | H356O128N24C40 | 7,07 | 0,8179 | -0,1002 |
| 14 | Water | H2O | 7,42 | 0,8040 | -0,1087 |
| 15 | Borax | Na2B4O17H20 | 8,06 | 0,7948 | -0,1143 |

*Table 1: R and M values for 2 cm material thickness under the emission spectrum of Figure 1.*

## Results

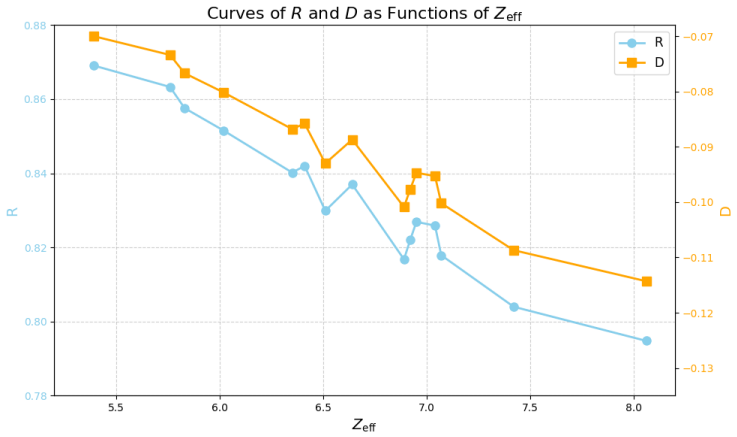


*Figure 2: Performance comparison of R and M, plotted from Table 1.*

Variations of R and M with $Z_{eff}$, shown in Figure 2, exhibit distinct trends across the organic material range ($Z_{eff}$ 5.4–8). The R curve (light blue) decreases quasi-linearly from 0.869 to 0.795, a 9.35% variation, indicating low sensitivity to $Z_{eff}$ changes. In contrast, the M curve (orange) declines more sharply from -0.070 to -0.114, a 63.2% variation, reflecting greater responsiveness. Consequently, a 1% deviation in measured attenuation coefficients impacts R more significantly than M due to M's normalization.

Relative error analysis, based on linear interpolation of the 15 data points, reveals higher precision for M (±3.51%) compared to R (±4.56%). This 1% error reduction underscores M's superior ability to capture energy-dependent attenuation variations in organic materials within the studied $Z_{eff}$ range. While not transformative, this improvement affirms M's robustness for applications requiring high precision.

## Discussion

M's slight superiority stems from its normalization, mitigating an offset that hampers R's extrapolation performance. Moreover, it demonstrates potential for compensating intrinsic measurement errors. Expressible as $M = \frac{1-R}{1+R}$, M exhibits lower error propagation than R, as derived from Gauss-Laplace:

$$\Delta M = \sqrt{(\frac{\partial f(\mu_1,\mu_2)}{\partial \mu_1}\,\Delta\mu_1)^2 + (\frac{\partial f(\mu_1,\mu_2)}{\partial \mu_2}\,\Delta\mu_2)^2} = \frac{2}{(1+R)^2}\,\Delta R,$$

where $R \in [0.7, 0.9]$, confirming $\Delta M < \Delta R$.

Despite M's advantages, combining R and M in a dual-metric approach refines $Z_{eff}$ estimates, leveraging R's simplicity and M's robustness. For instance, their joint use aids error interpretation: logarithmic regression can reveal whether $\mu_1$ or $\mu_2$ measurement errors dominate, based on the sign of the result. This could enhance $Z_{eff}$ estimation in airport baggage screening, where higher error at high energies might shift boundary classifications (e.g., organic green vs. inorganic orange), improving operator readability.

M's absence from the literature, despite its intuitive formulation, is noteworthy. Though novel in dual-energy X-ray imaging, it aligns with normalization heuristics in other imaging domains. This cross-disciplinary technique identification mirrors the TRIZ methodology, emphasizing interdisciplinary concept transfer.

## Conclusion

This note introduces a normalised metric $M = \frac{\mu_1-\mu_2}{\mu_1+\mu_2}$ for Zeff estimation in dual-energy X-ray imaging, and demonstrates a 23 % reduction in relative estimation error compared to the conventional attenuation ratio R, on analytical simulations over 15 organic materials. Error propagation analysis confirms that this improvement is structurally grounded: $\Delta M < \Delta R$ for the attenuation ratios typical of organic materials, regardless of the specific measurement conditions.

The broader observation this note intends to convey is methodological. The dual-energy X-ray community has invested heavily in reconstruction-side complexity over the past two decades, iterative solvers, regularisation schemes, basis decomposition algorithms, while the elementary question of how best to represent the two acquired measurements has received comparatively little attention. M, a metric borrowed from satellite remote sensing through a straightforward cross-disciplinary transposition, illustrates that meaningful gains remain accessible at the measurement representation level, without modifying acquisition hardware, increasing dose, or introducing computational overhead.

This does not diminish the value of more sophisticated approaches. It suggests, rather, that simple and complex methods are not mutually exclusive: an improved base metric such as M can serve as input to any downstream algorithm, potentially amplifying the gains of methods that build upon it. Experimental validation on physical dual-energy systems is the natural next step to confirm these analytical findings.

**References**

[1] Alvarez, R. E., & Macovski, A. (1976). Energy-selective reconstructions in X-ray computerized tomography. Physics in Medicine & Biology, 21(5), 733–744. DOI: 10.1088/0031-9155/21/5/002

[2] Jia Hao et al. (2013). A novel image optimization method for dual-energy computed tomography. Nuclear Instruments and Methods in Physics Research A, 722, 34–42. DOI: 10.1016/j.nima.2013.04.080

[3] Lehmann, L. A., et al. (1981). Generalized image combinations in dual kVp digital radiography. Medical Physics, 8(5), 659–667. DOI: 10.1118/1.595025

[4] Yalçın, O. (2022). Detection of explosive materials in dual-energy X-ray security systems. Journal of Instrumentation, 17(10), P10012. DOI: 10.1088/1748-0221/17/10/P10012

[5] US Patent US20110150183A1, "Dual-energy imaging at reduced sample rates," 2011.

[6] Berger, M. J., et al. NIST, PML, Radiation Physics Division.

[7] Ying, Z., Naidu, R., & Crawford, C. R. (2006). Dual energy computed tomography for explosive detection. Journal of X-Ray Science and Technology, 14, 235–256.

[8] Patent Wang et al., US 20070286329, "Energy spectrum apparatus, material discrimination method and device, image processing method," 2007.